Med Chem Res
DOI 10.1007/s00044-015-1363-3

MEDICINAL CHEMISTRY RESEARCH

ORIGINAL RESEARCH

Cytotoxic activities and metabolic studies of new combretastatin analogues

Yohan Macé[1] · Emilie Bony[2] · David Delvaux[3] · Adan Pinto[3] · Véronique Mathieu[4] · Robert Kiss[4] · Olivier Feron[3] · Joëlle Quetin-Leclercq[2] · Olivier Riant[1]

Received: 3 November 2014 / Accepted: 10 March 2015

Abstract A new series of combretastatin analogues with B-ring modifications were synthesized and evaluated for their cytotoxicity against one endothelial (HUVEC) and three tumor cell lines, e.g., the LoVo colon, the PC-3 prostate, and the U373 glioma cancer models. These new combretastatin analogues showed differential cytotoxic activities, *cis* derivatives **13** 5-(2-*Z*-trimethoxyphenylethenyl)-benzo[1,2-c]1,2,5-oxadiazole N^1-oxide and **14** 5-(2-*Z*-trimethoxyphenylethenyl)benzo[1,2,5]thiadiazole exhibiting interesting cytotoxicity both on endothelial and on tumor cells. Unlike the *cis* benzofurazan **12** 5-(2-*Z*-trimethoxyphenylethenyl)benzo[1,2-c]1,2,5-oxadiazole, induction of apoptosis by **13** appeared to be through caspase-3 activation. Metabolic investigations showed a positive correlation between highly metabolized compounds and cytotoxic activity, suggesting that highly cytotoxic derivatives may act as pro-drug via a reductive metabolization to more active metabolites.

Keywords Benzofuroxan derivates · Benzothiadiazole · Cytotoxicity · Metabolism · Stilbenes

Yohan Macé and Emilie Bony have contributed equally to this work.

Electronic supplementary material The online version of this article (doi:10.1007/s00044-015-1363-3) contains supplementary material, which is available to authorized users.

✉ Olivier Feron
olivier.feron@uclouvain.be

✉ Olivier Riant
olivier.riant@uclouvain.be

[1] Institute of Condensed Matter and Nanosciences Molecules, Solids and Reactivity (IMCN/MOST), Université catholique de Louvain, Louvain-la-Neuve, Belgium

[2] Pharmacognosy Research Group (GNOS), Louvain Drug Research Institute (LDRI), Université catholique de Louvain, Brussels, Belgium

[3] Pole of Pharmacology and Therapeutics (FATH), Institut de Recherche Expérimentale et Clinique (IREC), Université catholique de Louvain, Brussels, Belgium

[4] Laboratoire de Cancérologie et de Toxicologie Expérimentale, Faculté de Pharmacie, Université Libre de Bruxelles, Brussels, Belgium

Introduction

Combretastatin initially isolated and characterized by Pettit et al. from the bark of South African tree *Combretum caffrum* is known for its anti-tumor activity due to its anti-tubulin properties (Simoni *et al.*, 2006). It also showed cytotoxic (Cushman *et al.*, 1992; Pettit *et al.*, 1995a) and anti-angiogenic (Dark *et al.*, 1997; Liekens *et al.*, 2001) activities, but its major drawback is its low solubility. The ability to create strong damage in tumor cells and structural simplicity of CA-4 **1,** a combretastatin analogue (Fig. 1), stimulated the search of new and more efficient compounds with better pharmacological properties. Many efforts have led to the preparation of more soluble analogues (Bedford *et al.*, 1996), for example, combretastatin CA-4 phosphate (CA-4P) **2** or amine **3** pro-drugs (Pettit *et al.*, 1995b). They exert antineoplastic activity through disruption of the blood flow within the tumor leading to tumor cell death (Chaplin and Dougherty, 1999). In particular, the water soluble CA-4P has shown great clinical promise. In a phase I clinical trial, 15 patients with advanced cancer received CA-4P with bevacizumab, and this combination appeared safe and well tolerated. It was shown in this study that CA-4P induced profound vascular changes, which were maintained by the presence of bevacizumab (Nathan *et al.*, 2012). In a

Published online: 09 April 2015

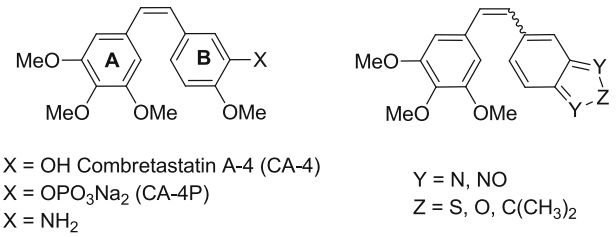

Fig. 1 Chemical structures of combretastatin A-4 and studied analogues

phase II trial on 44 patients with platinum-resistant ovarian cancer, the addition of CA-4P to paclitaxel and carboplatin was well tolerated and appeared to produce a higher response rate in this patient population than if the chemotherapy was given without CA-4P (Zweifel *et al.*, 2011). In addition to their effect on the vasculature network within the tumors, it was shown that CA-4P as well as other *cis*-combretastatin A-4 derivatives had a strong inhibition activity on several cancer cell lines including multi-drug-resistant cells (Dark *et al.*, 1997). However, these new analogues were found to have significant side effects such as cardiovascular toxicity and neurotoxicity (Rustin *et al.*, 2003). For these reasons, it is necessary to elaborate new and more specific combretastatin analogues for tumor and endothelial cells. Previous structure–activity relationship (SAR) studies established that the *cis*-configuration of the double bond and the methoxy groups in position 3, 4, and 5 in the A-ring and position 4′ in the B-ring is essential for an actual biological activity (Nam, 2003). In order to optimize both their activity on tumor and endothelial cells, we synthesized new combretastatin derivatives that cover a wide range of chemical structures.

We maintained the 3,4,5-trimethoxy-substituted pattern on A-ring and examined the effects due to replacement of the B-ring with different benzoheterocycles. Recently, Simoni et al. examined the effects regarding replacement of the B-ring of CA-4 with benzofuran or benzothiophene (Simoni *et al.*, 2006; Simoni *et al.*, 2008). These compounds possess potent cytotoxic activity while also showing potent binding to tubulin and inhibition of tubulin polymerization. In this study, we investigated stilbenes by extending the replacement of the B-ring by a new class of benzoheterocycle pro-drugs such as benzofuroxan, benzofurazan, or benzothiadiazole (Fig. 2).

The present report summarizes the synthesis of *cis*- and *trans*-stilbenes of these new types of combretastatin analogues. We analyzed the in vitro activity of the synthesized compounds on endothelial and cancer cell lines and showed that some molecules exert both a very strong anti-angiogenic (inhibition of endothelial cell growth) and anti-tumoral (inhibition of cancer cell growth) effects. The pro-apoptotic effect of the most active derivatives was also analyzed. Then, we performed metabolism investigations to determine whether these compounds act directly or via metabolites. Metabolites formed by in vitro microsomal degradation were analyzed by high-performance liquid chromatography (HPLC). Structural determination of metabolites was realized by high-resolution mass spectrometry (HRMS) and by LC–MS comparison with authentic standards of expected metabolites whose synthesis is described here.

Results and discussion

Chemistry

The synthetic route to obtain the combretastatin analogues is described in Scheme 1. Trimethoxybenzyltriphenylphosphonium bromide was synthesized from corresponding aldehyde by reduction with $NaBH_4$ followed by an exchanging of alcohol by bromide with PBr_3 as reported in the literature. The last step consists in the formation of phosphonium salt in the presence of triphenylphosphine in tetrahydrofuran (THF) (Maya *et al.*, 2005).

The 5-formylbenzofuroxan was easily synthesized in one-pot process from 4-chloro-3-nitrobenzaldehyde via S_NAr with azide and subsequent cyclization in dimethyl sulfoxide (DMSO) (Scheme 2) (Porcal *et al.*, 2008). The 5-formylbenzothiadiazole **7** was prepared from the commercially available methyl-3,4-diaminobenzoate **4**, which was treated with thionyl chloride in the presence of triethylamine in dichloromethane (DCM) as solvent, affording the corresponding benzothiadiazole **5** (DaSilveira Neto *et al.*, 2005). Reaction with LiI in pyridine and subsequent esterification/reduction in the presence of *N,N*-diisopropylethylamine (DIPEA) and ClCOOEt following a treatment with $NaBH_4$ led to benzothiadiazol-5-ylmethanol **6** (Poulain *et al.*, 2001), which can be oxidized to the corresponding aldehyde **7** with MnO_2 (Carroll *et al.*, 2004).

Wittig reaction between phosphonium bromides and the different aryl aldehydes was carried out in THF with potassium bis(trimethylsilyl)amide (KHMDS) in the presence of hexamethylphosphoramide (HMPA) (Scheme 1). Use of KHMDS as the base and HMPA as chelating agent gave the best results of desired *Z*-isomers with a *Z/E* ratio of 60:40. The mixture of the *Z* and *E* stilbene isomers was separated using flash column chromatography, leading to the corresponding *cis*-stilbenes and *trans*-stilbenes identified by the difference of the coupling constants of vinylic proton in NMR (around 12 Hz for *Z*-isomers and 16 Hz for *E*-isomers).

Finally, the other analogues were prepared directly from the benzofuroxan stilbenes (Scheme 2). The use of triphenyl phosphine in the presence of ethanol led to the

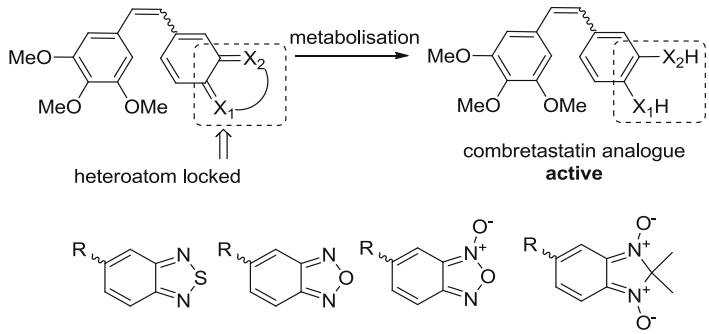

Fig. 2 Heterocyclic derivates of combretastatin

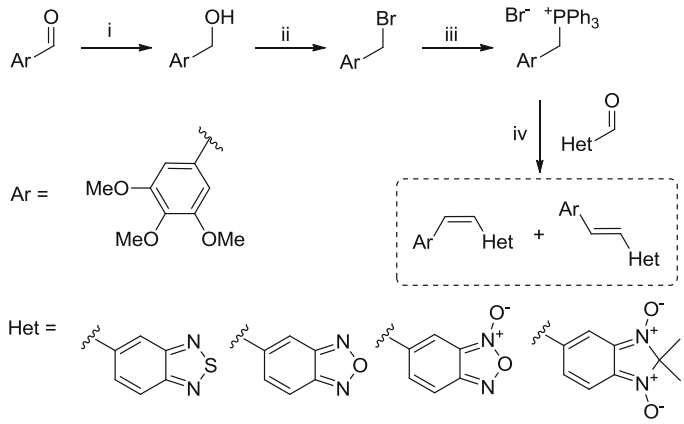

Scheme 1 General pathway for the preparation of stilbenes. *i* $NaBH_4$, MeOH; *ii* PBr_3, DCM; *iii* PPh_3, THF; *iv* KHMDS, HMPA/THF

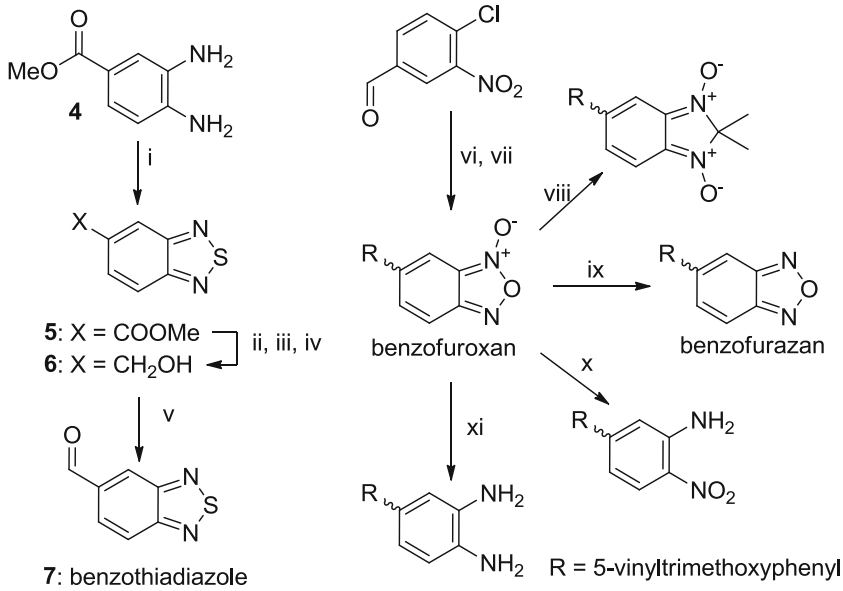

Scheme 2 Synthesis of heterocyclic compounds. *i* $SOCl_2$, Et_3N, DCM; *ii* LiI, pyridine; *iii* DIPEA, ClCOOEt, THF; *iv* $NaBH_4$, H_2O; *v* MnO_2, $CHCl_3$; *vi* NaN_3, DMSO; *vii* Arylphophosnium bromide salt, KHMDS, HMPA/THF; *viii* 2-nitropropane, piperidine, THF; *ix* PPh_3, EtOH; *x* $FeSO_4.7H_2O$, DMSO; *xi* $SnCl_2{\cdot}H_2O$, AcOEt

deoxygenation of benzofuroxan in benzofurazan (Aguirre *et al.*, 2005). The formation of benzimidazole dioxide was obtained following the Abu El-Haj (Abu El-Haj, 1972) method using 2-nitropropane in the presence of piperidine as base in THF (Boiani *et al.*, 2006).

Some of the expected metabolites of heterocyclic derivates of combretastatin (Scheme 3) were synthesized to afford references for the metabolic investigations. Only the metabolites from the reduction process were prepared following two different methods (other metabolites were already prepared by the reaction described above). On the one hand, the reduction of benzofuroxan was performed with $FeSO_4$ in ethyl acetate (AcOEt) to obtain the corresponding nitro amine stilbenes (Porcal *et al.*, 2008), on the

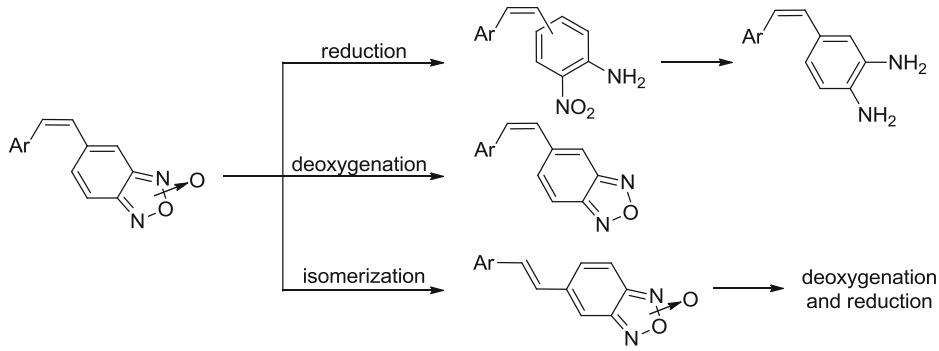

Scheme 3 Some of the expected metabolites

other hand with $SnCl_2$ in DMSO to obtain the diamine stilbene (Scheme 3).

Biological studies

For most products of the two groups **8–11** and **12–15**, we did not observe striking differences regarding the cytotoxicity (IC_{50}) between HUVEC cells and cancer cells (Table 1). We nevertheless observed a higher activity on HUVEC cells for **14**. The group **12–15** contains the more active products; their IC_{50} are distributed on a 3 log order range. Previously reported importance of *cis*-configuration was only observed here with benzofuroxan and 2,1,3-benzothiadiazole substitutions. **3** was used as reference compound since this combretastatin analogue already showed potent anti-tumor activity in vitro and in vivo (Ohsumi *et al.*, 1998).

Pro-apoptotic effects

Within the most active group (*cis*-stilbenes), we decided to investigate the pro-apoptotic effect of **13**, a highly cytotoxic derivative, compared to **12**, that is less cytotoxic, and **3** which is used as a reference compound. Internucleosomal DNA fragmentation is one of the hallmarks of apoptosis that occurs after the final lytic event (Collins *et al.*, 1997). To quantitate the relative proportion of apoptotic population of cells following a 72-h treatment with **12**, **13**, and **3**, U373 glioma cells were analyzed by flow cytometry after propidium iodide and TUNEL staining. As shown in Fig. 3, the apoptotic population, as indicated by pre-G1 phase, was much higher in treated cells than in control.

TUNEL staining confirmed that **12**, **13**, and **3** does indeed induce apoptosis in U373 glioma cells (Fig. 4a). In contrast to propidium iodide staining, TUNEL assay nevertheless highlighted a dose-dependent apoptotic response in U373 cells treated with **13,** which is not the case with **12** and **3**. To determine the mechanism of apoptosis-induced effects, we also analyzed caspase-3 activation (Jänicke *et al.*, 1998). The differential effect between **13** and the other tested compounds is probably due to the fact that **13** is the only compound that induces apoptosis through caspase-3 activation (Fig. 4b).

Metabolic stability studies

To determine whether the synthesized compounds were effective as such or via metabolites on cell proliferation, and to try to explain the observed cytotoxic effects, we evaluated the phase I metabolism of stilbenes both on

Table 1 Cytotoxic activity (IC_{50} μM) of the compounds

Compound	A-ring	B-ring	HUVECs	LoVo	PC-3	U373
8	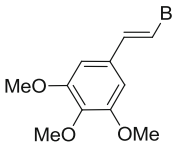	Benzofurazan	>100	37	83	43
9		Benzofuroxan	60	3	6	10
10		2,1,3-benzothiadiazole	87	38	88	>100
11		2,2-dimethyl-benzimidazole dioxide	4.3	4	7	4
12		Benzofurazan	30	24	61	30
13		Benzofuroxan	1.5	0.5	2	0.9
14	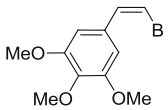	2,1,3-benzothiadiazole	0.1	1	7	3
15		2,2-dimethyl-benzimidazole dioxide	6.2	4	19	5
3[a]		4-methoxy-3-aminobenzene	0.02	<0.01	<0.01	<0.01

[a] Reference compound

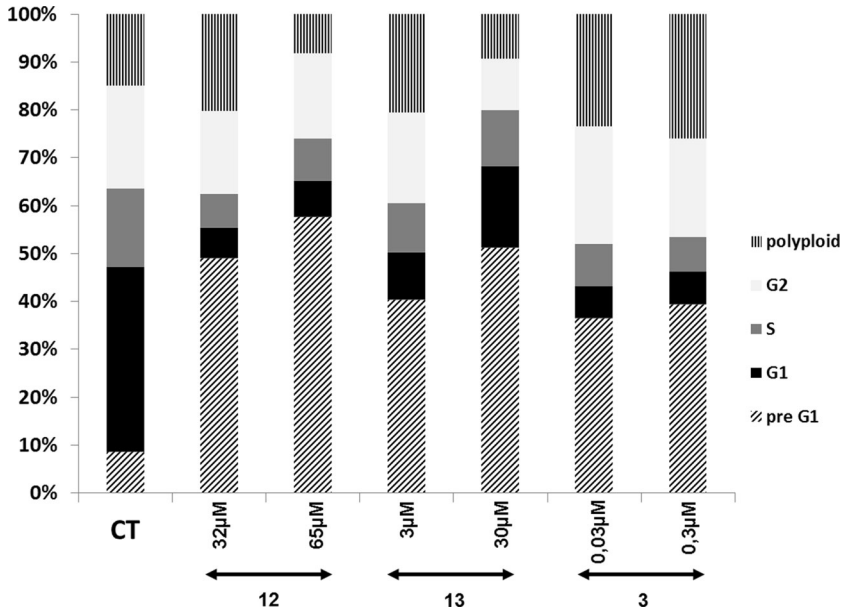

Fig. 3 Pre-G1 accumulation of U373 glioma cells after 72-h treatment with **12**, **13**, and **3**

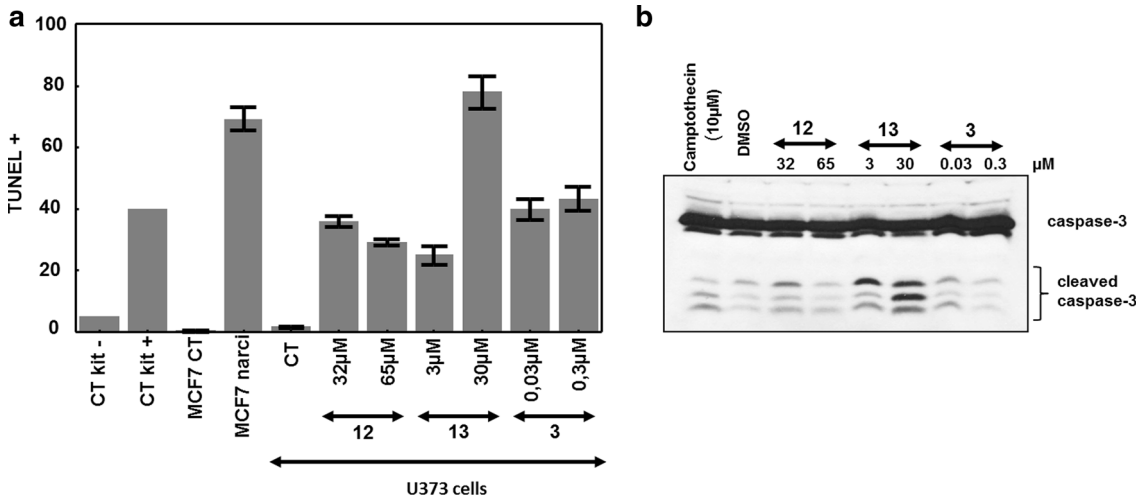

Fig. 4 **a** TUNEL; **b** Immunoblot of caspase-3 cleavage in U373 cells following 24 h of treatment with different concentrations of the indicated compounds

mouse liver and on human liver S9 microsomes. On mouse liver microsomes, most tested compounds showed a rapid degradation with $t_{1/2}$ from 0.1 to 6.0 min, **8** and **10** with $t_{1/2}$ of 13.4 and 10.8 min, respectively, being the more stable compounds. On human liver S9 microsomes, all compounds appeared more stable and **8** and **10** exhibited again a better metabolic stability profile with $t_{1/2}$ of 114 and 73.6 min, respectively (Table 2). Interestingly, **8** and **10** which are the more stable compounds in this study also showed the lowest cytotoxicity. As metabolization in cultured cells is much slower than on purified microsomes, it is possible that produced metabolites are responsible for cytotoxic activities of highly metabolized compounds such as **13** and **14,** which would not be the case with slowly metabolized compounds.

In order to see whether a correlation exists between cytotoxic activity and metabolization for **8–15** derivatives, metabolite identification was performed by HPLC–Orbitrap–MS (Table 3) by comparing retention times and MS^2 mass spectra with expected reduced metabolites (**16**, **17**, **18**, **19**, and **20**). Cytotoxic activity of synthesized metabolites was also investigated, and the data are given in Table 4.

HPLC–MS profiles of furazan metabolites (**8** and **12**) only revealed the presence of oxidized metabolites. Metabolization of **8** only produced an unstable metabolite at *m/z* 347.1226 corresponding to $[C_{17}H_{19}N_2O_6]^+$ ($[M+H]^+$

Table 2 Stability ($t_{1/2}$ and CL_{int}) of combretastatin analogues both in mouse liver microsomes and in human liver S9

Compound	Mouse liver microsomes		Human liver S9	
	$t_{1/2}$ (min)	CL_{int} (mL/min/g)	$t_{1/2}$ (min)	CL_{int} (mL/min/g)
8	13.4	51.7	114	6.1
9	6	115.5	13.8	50.2
10	10.8	64.2	73.6	9.4
11	1.3	533.1	5.2	133.3
12	1.7	407.6	44.5	15.6
13	0.1	6930.0	3.2	216.6
14	0.1	6930.0	16.3	42.5
15	1.9	364.0	8.9	77.9

$n = 2$ for each compound

$t_{1/2}$: half-life of the drug; CL_{int} intrinsic clearance

calcd: 347.1238), which probably results from the oxidation of the furazan group, whereas produced metabolites from **12** corresponded to several demethylated metabolites at *m/z* 299.1018 and hydroxylated metabolites at *m/z* 329.1121 with raw formula $[C_{16}H_{15}N_2O_4]^+$ ($[M+H]^+$ calcd: 299.1026) and $[C_{17}H_{17}N_2O_5]^+$ ($[M+H]^+$ calcd: 329.1132), respectively.

The metabolization of benzofuroxans produced both oxidized and reduced metabolites. By comparison with expected metabolites, HPLC–MS profile of **9** allowed us to identify two reduced metabolites **16** and **17**, **16** being the main metabolite, and an oxidized metabolite at *m/z* 347.1217 corresponding to $[C_{17}H_{19}N_2O_6]^+$ ($[M+H]^+$ calcd: 347.1238), the same metabolite as **8**. The metabolization of **13** produced oxidized metabolites at *m/z* 333.1067 and m/z 317.1120 corresponding to demethylated ($[C_{16}H_{17}N_2O_6]^+$, $[M+H]^+$ calcd: 333.1081) and hydroxylated metabolites ($[C_{16}H_{17}N_2O_5]^+$, $[M+H]^+$ calcd: 317.1132). Moreover, four reduced metabolites have been identified: **16**, **18**, **19**, and **20**, with **18** being the main metabolite. It appeared that the higher cytotoxicity of **13** compared to **9** may be explained by its fast reduction to more cytotoxic *cis* metabolites, i.e., **18**, **19**, and **20** as illustrated in Fig. 5 and Table 4. Indeed, **18** and **19** are rapidly observed since they already appeared on the chromatogram at 0 min of incubation (directly when the compound is solubilized).

Compounds **11** and **15** showed similar cytotoxicity and metabolic stability. However, HPLC–MS metabolite profile of **11** showed only the reduced metabolite **17**, whereas **15** metabolization produced two reduced metabolites **17** and **20**, and various primary or secondary oxidized metabolites at *m/z* 285.1223, 287.1377, 341.1482, and 355.1637 correspond to $[C_{16}H_{17}N_2O_3]^+$ ($[M+H]^+$ calcd: 285.1234), $[C_{16}H_{19}N_2O_3]^+$ ($[M+H]^+$ calcd: 287.1390), $[C_{19}H_{21}N_2O_4]^+$ ($[M+H]^+$ calcd: 341.1496), and $[C_{20}H_{23}N_2O_4]^+$ ($[M+H]^+$ calcd: 355.1652), respectively. Even if **20** is the major metabolite produced, other identified compounds still represent a significant proportion of produced metabolites.

The metabolization of thiadiazole isomers **10** and **14** is similar to **11** and **15**. Indeed, **10** metabolization produced

Table 3 Major identified metabolites of combretastatin analogues by HPLC–Orbitrap–HRMS (*m/z* at 10 mmu) and relative intensities after 60-min incubation with mouse liver microsomes

Compound	Tr[a] (min)	$[M+H]^+$	Identified compounds *m/z* (relative intensity %)
8	16.4	313.1170	313.1226 **8** (10.6), 347.1226 (100)
9	15.8	329.1115	301.1531 **17** (78.4), 331.1271 **16** (100), 347.1217 (2.7)
10	17.1	329.0941	301.1532 **17** (100), 329.0941 **10** (23.8)
11	9.9	371.1585	301.1530 **17** (100)
12	16.1	313.1171	299.1018, 329.1121 (100)
13	15.5	329.1121	301.1535 **20** (5.3), 317.1120 (26.5), 331.1278 **16** (2.2), 331.1277 **18** (100), 331.1277 **19** (0.3), 333.1067 (4.1)
14	16.8	329.0941	315.0787 (7.3), 301.1535 **17** (5.5), 301.1534 **20** (100), 363.0996 (16.5)
15	9.8	371.1585	285.1223 (5.7), 287.1377 (44.0), 301.1534 **17** (33.1), 301.1535 **20** (100), 341.1482 (36.1), 355.1637 (42.9)

[a] Retention time of initial compounds obtained by HPLC–UV

Table 4 Cytotoxic activity (IC_{50} μM) of reduced metabolites

Compound	A-ring	B-ring	HUVECs	LoVo	PC-3	U373
16[a]	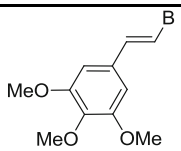	3-Nitro-4-aminobenzene	46	24	22	38
17		3,4-Diaminobenzene	3.7	4	5	4
18		3-Nitro-4-aminobenzene	0.08	0.05	0.23	0.15
19		4-Nitro-3-aminobenzene	0.6	0.6	9	0.7
20	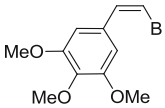	3,4-Diaminobenzene	1.1	0.3	1.2	0.5

[a] Ratio 72/28 3-nitro-4-aminobenzene/4-nitro-3-aminobenzene

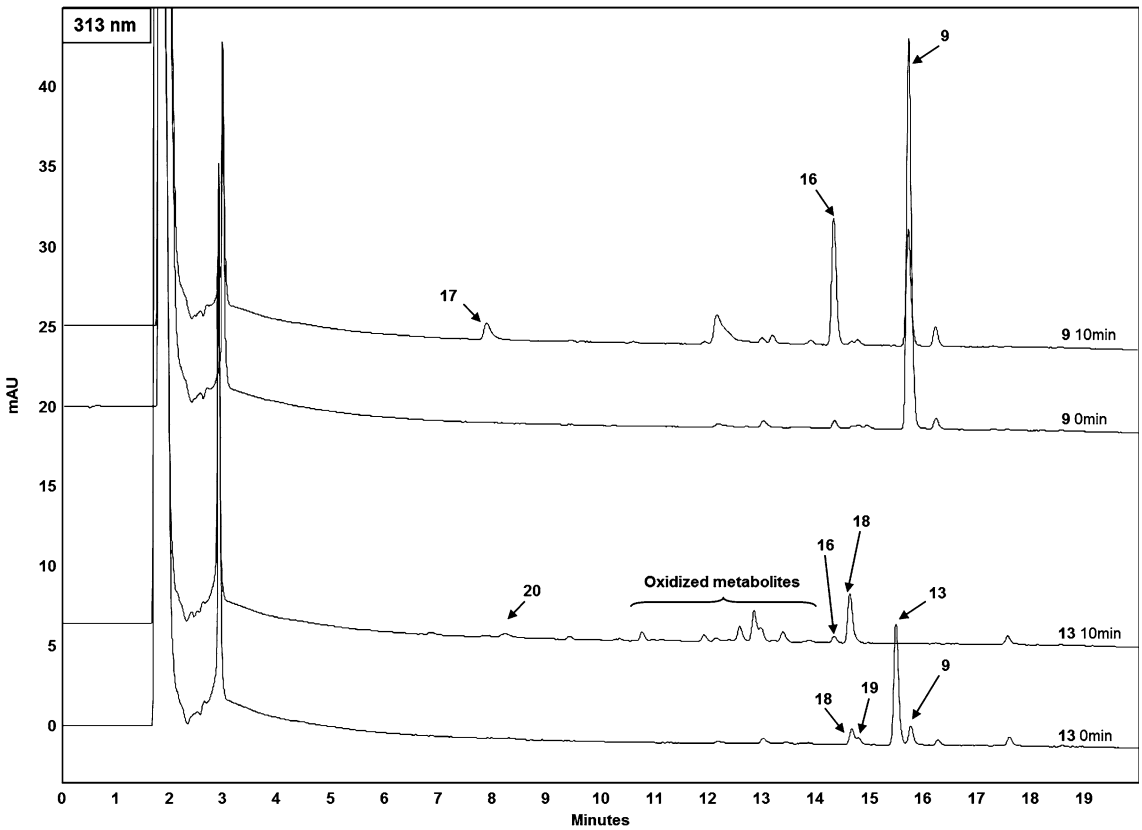

Fig. 5 Comparison of obtained chromatograms from **9** to **13** in the presence of mouse liver microsome at 0 and after 10-min incubation (detection at 313 nm)

the reduced metabolite **17**, whereas the metabolization of **14** produced diverse oxidized metabolites and the reduced metabolites **17** and **20**; unlike **15**, the main metabolite of **14** is **20**, which is much cytotoxic than **17**. The oxidized metabolites identified at *m/z* 315.0787 and 363.0996 correspond to $[C_{16}H_{15}N_2O_3S_1]^+$ ($[M+H]^+$ calcd: 315.0798) and $[C_{17}H_{19}N_2O_5S_1]^+$ ($[M+H]^+$ calcd: 363.1009), respectively. However, the *cis*-isomer **14** is much more cytotoxic than the *trans*-isomer **10**. This difference may be due to the good metabolic stability of **10** compared to **14**, which is very unstable, leading rapidly to the production of the more cytotoxic major metabolite **20** as shown in Table 4.

Conclusion

In this study, we reported the synthesis of new combretastatin analogues by replacing the B-ring with different benzofuroxan and benzothiadiazole derivatives as well as

reduced metabolites and analyzed their cytotoxic activity on one endothelial and three tumor cell lines. We also determined their metabolic stability and identified metabolites by LC-HRMS. Two newly synthesized derivatives **13** and **14** exhibited interesting levels of cytotoxicity both on endothelial and on tumor cells, with **14** being more toxic to HUVEC cells showing a higher anti-angiogenic potential. We also showed that these compounds possess pro-apoptotic properties and that the mode of induction of apoptosis could differ according to the chemical structure. In fact, we showed that **13** induced apoptosis through caspase-3 activation, whereas the less cytotoxic derivative of this series **12** and the reference compound **3** did not induce apoptosis through this pathway.

Investigation of metabolic stability indicated that the most cytotoxic *cis* compounds **13** and **14** are rapidly metabolized to more cytotoxic reduced *cis* derivatives, whereas the less cytotoxic *trans* compounds **9** and **10** appeared more stable both on human and on mouse microsomes and also produced less cytotoxic *trans* metabolites. These results indicated that some of these compounds may act as pro-drug via reductive activation and that highly cytotoxic *cis*-configuration can be maintained during reductive metabolization.

Experimental

Chemistry

All starting materials were purchased from commercial suppliers (Acros, Sigma-Aldrich, ABCR or TCI) and used without further purification. Solvent used was anhydrous, and the reactions were carried out under an argon atmosphere using standard glassware. ^{1}H and ^{13}C spectra were recorded on a Brucker-300 MHz spectrometer. Chemical shifts for ^{1}H and ^{13}C NMR acquired in $CDCl_3$ are reported in ppm relative to residual solvent proton ($\delta = 7.26$ ppm) and carbon ($\delta = 77$ ppm) signals, respectively. Multiplicity is indicated follows: s (singlet); d (doublet); t (triplet); m (multiplet); dd (doublet of doublet); ddd (doublet of doublet of doublet); and br (broad). Coupling constants are reported in hertz (Hz). High- and low-resolution mass spectra were acquired using electrospray as the ionization technique in positive ion mode as stated all MS analysis samples were prepared as solutions in methanol. Column chromatography was carried out on silica gel (ROCC 60, 40–63 µm). TLC analyses were performed on commercial aluminium plates bearing a 0.25-mm layer of Merck Silica gel $60F_{254}$. The purity of all biologically evaluated compounds was confirmed to be >95 % by HPLC. Combretastatin analogue **3** was prepared by the method as reported in the literature (Ohsumi *et al.*, 1998) copy of ^{1}H and ^{13}C NMR spectra are given in the electronic supplementary material.

5-Formylbenzo[1,2-c]1,2,5-oxadiazole N-Oxide A mixture of 4-chloro-3-nitrobenzaldehyde (1.9 g, 10.3 mmol) and NaN_3 (0.63 g, 9.7 mmol) in DMSO (12 mL) was heated at 75 °C during 30 min and subsequently at 100 °C during 1.5 h. The residue was diluted with H_2O (20 mL) and extracted with EtOAc (3 × 10 mL). After the workup, the organic layer was dried with $MgSO_4$ and evaporated in vacuum. The residue was purified by chromatographic column (DCM) to give a yellow solid (1.65 g, 98 %).^{1}H NMR (300 MHz, $CDCl_3$) δ 10.00 (s, 1H), 7.95 (br s, 1H), 7.83 (br s, 1H), 7.71 (br s, 1H).

3,4-Diaminobenzoic acid methyl ester (**4**) H_2SO_4 (6 mL, 113 mmol) was slowly added dropwise at 0 °C to a solution of 3,4-diaminobenzoic acid (3 g, 19.7 mmol) in methanol (60 mL) with stirring; then, the mixture heated at reflux for 3 h. Saturated solution of $NaHCO_3$ was added until the mixture was basic; then, the mixture was extracted with DCM. The extract was dried and evaporated in vacuum to give the product **4** (2.98 g, 91 %) as a brown crystalline solid. ^{1}H NMR (300 MHz, $CDCl_3$) δ 7.46 (dd, $J = 8.1$, 1.8 Hz, 1H), 7.41 (d, $J = 1.8$ Hz, 1H), 6.67 (d, $J = 8.1$ Hz, 1H), 3.85 (s, 3H), 3.53 (s, 4H).

Benzo[1,2,5]thiadiazole-5-carboxylic acid methyl ester (**5**) 3,4-Diaminobenzoic acid methyl ester **4** (1.5 g, 9 mmol) was added to a solution of DCM (50 mL) and triethylamine (5.1 mL, 36.6 mmol). The solution was stirred until total dissolution of the diamine. Then, thionyl chloride (1.32 mL, 18 mmol) was added dropwise very slowly, and the mixture refluxed for 4 h. The solvent was removed under reduced pressure and 20 mL of water added. Concentrated HCl was added at 0 °C until pH = 2. Then, the mixture was extracted with DCM (3 × 20 mL), dried over $MgSO_4$, and filtered. The solvent was removed, affording pure compound **5** in quantitative yield (1.75 g). ^{1}H NMR (300 MHz, $CDCl_3$) δ 8.76 (d, $J = 0.6$ Hz, 1H), 8.22 (dd, $J = 9.3$, 1.3 Hz, 1H), 8.05 (d, $J = 9.2$ Hz, 1H), 4.01 (s, 3H).

Benzo[1,2,5]thiadiazol-5-ylmethanol (**6**) A mixture of benzo[1,2,5]thiadiazole-5-carboxylic acid methyl ester **5** (1.75 g, 9 mmol) in pyridine (25 mL) and LiI (7.25 g, 54.2 mmol) was refluxed overnight. The solvent was removed under reduced pressure, and the resulting oil was dissolved in H_2O (25 mL). After the addition of HCl (3 N) at 0 °C, the mixture was extracted with DCM (3 × 25 mL), dried over $MgSO_4$, and filtered. The solvent was removed. The resulting solid was dissolved in THF (30 mL) and DIPEA (1.8 mL, 10.33 mmol). The mixture was cooled to 0 °C, and ClCOOEt (1 mL, 10.46 mmol) was added. After the resulting mixture was stirred for 1.5 h

at 0 °C, a solution of $NaBH_4$ (0.8 g, 21.14 mmol) in H_2O (4 mL) was added dropwise. The mixture was stirred for 2 h at room temperature and evaporated under reduced pressure. The orange residue was dissolved in AcOEt (20 mL) and washed with a saturated solution of Na_2CO_3 (20 mL) and brine (20 mL). The organic layer was dried over $MgSO_4$, filtered, evaporated under reduced pressure, and purified by flash chromatography (petroleum ether/AcOEt 5:5 to AcOEt) to yield 1.06 g (71 %) of **6** a yellow powder. ^{1}H NMR (300 MHz, $CDCl_3$) δ 7.84 (s, 1H), 7.83 (d, $J = 9.1$ Hz, 1H), 7.46 (dd, $J = 8.9$, 1.7 Hz, 1H), 4.80 (br s, 2H), 3.42 (br s, 1H).

Benzo[1,2,5]thiadiazol-5-carboxaldehyde (**7**) Benzo[1,2,5]thiadiazol-5-ylmethanol **6** (115 mg, 0.69 mmol) and MnO_2 (241 mg, 2.8 mmol) in $CHCl_3$ (10 mL) were stirred at room temperature overnight. The reaction mixture was filtered on a plug of Celite and the filtrate evaporated to provide 111 mg of pure 2,1,3-benzothiadiazole-5-carboxaldehyde **7** (98 %): ^{1}H NMR (300 MHz, $CDCl_3$) δ 10.19 (s, 1H), 8.49 (s, 1H), 8.09 (s, 2H).

3,4,5-Trimethoxybenzyl alcohol 3,4,5-Trimethoxybenzaldehyde (5 g, 25.5 mmol) was dissolved in methanol (50 mL) and cooled to 0 °C. $NaBH_4$ (1.45 g, 38 mmol) was added in small portion. Then, the reaction mixture was stirred 1 h at room temperature. The solvent was removed under reduce pressure, and the crude was diluted in water (20 mL) and extracted with AcOEt (3 × 20 mL). The organic phases were combined, dried over $MgSO_4$, filtered, and concentrated to give colorless oil in quantitative yield (5.05 g, 25.5 mmol). ^{1}H NMR (300 MHz, $CDCl_3$) δ (ppm): 6.60 (s, 2H), 4.63 (d, $J = 5.4$ Hz, 2H), 3.86 (s, 6H), 3.83 (s, 3H).

3,4,5-Trimethoxybenzyl bromide 3,4,5-Trimethoxybenzyl alcohol (5.05 g, 25.5 mmol) was diluted in dry DCM (20 mL) and cooled to 0 °C. PBr_3 (2.5 mL, 26.3 mmol) was added dropwise. The mixture was stirred 2 h at room temperature, poured onto water (20 mL), and extracted with DCM (3 × 20 mL). The organic layer was dried over $MgSO_4$ and evaporated under reduce pressure to give white solid in quantitative yield (6.66 g, 25.5 mmol). ^{1}H NMR (300 MHz, $CDCl_3$) δ (ppm): 6.58 (s, 2H), 4.42 (s, 2H), 3.82 (s, 6H), 3.80 (s, 3H).

3,4,5-Trimethoxybenzyltriphenylphosphonium bromide Triphenylphosphine (10.5 g, 30.6 mmol) and 3,4,5-trimethoxybenzyl bromide (6.66 g, 25.5 mmol) were dissolved in 60 mL of THF. The mixture was refluxed with stirring overnight. The resulting white solid was filtered and washed with hexane to afford the phosphonium salt in 91 % yield (12.5 g). ^{1}H NMR (300 MHz, $CDCl_3$) δ 7.80–7.70 (m, 9H), 7.65–7.54 (m, 6H), 6.47 (d, $J = 2.5$ Hz, 2H), 5.39 (d, $J = 14.1$ Hz, 2H), 3.75 (s, 3H), 3.49 (s, 6H).

*General procedure for Wittig reactions (**9**, **10**, **13** and **14**)*

The required phosphonium bromide (ca. 0.1 M) was suspended in dry THF and cooled to 0 °C under Ar. KHMDS (0.7 M in toluene 1.1 equiv) was added dropwise, and the resulting solution was stirred at room temperature for 1 h. Then, dry HMPA (2 equiv) was added, and the mixture was stirred at the same temperature for an additional 30 min. Then, a solution of aldehyde (1 equiv) in THF (ca. 0.2 M) was added dropwise at −78 °C. The mixture was stirred overnight at room temperature, quenched with 10 mL of aqueous solution of $NaHCO_3$ (5 %), and extracted with AcOEt (3 × 20 mL). The organic layer was dried over $MgSO_4$ and evaporated under reduce pressure. The residue was purified with flash chromatography on silica gel using petroleum ether and AcOEt as eluant to afford the *E*- and *Z*-isomers in variable yields.

5-(2-Z-Trimethoxyphenylethenyl)benzo[1,2-c]1,2,5-oxadiazole N^1-oxide (**13**) *and 5-(2-E-Trimethoxyphenylethenyl)benzo[1,2-c]1,2,5-oxadiazole N^1-oxide* (**9**) Purification by flash chromatography (PE/AcOEt, 80:20) afforded 87 % yield of separable isomers *Z/E* (56/44 ratio). **13** (*Z*-isomer): ^{1}H NMR (300 MHz, $CDCl_3$) δ 7.49–7.01 (m, 3H), 6.77 (d, $J = 12.2$ Hz, 1H), 6.53 (d, $J = 12.1$ Hz, 1H), 6.45 (s, 2H), 3.86 (s, 3H), 3.71 (s, 6H); ^{13}C NMR (75 MHz, $CDCl_3$) δ 153.18, 138.18, 134.34, 131.29, 126.91, 106.17, 60.93, 56.01; MS (APCI) *m/z:* 301.1 ($[M4H-2O]^+$), 314.1 ($[M2H-O)^+]$, 329.1 ($[MH]^+$); HRMS calcd for $C_{17}H_{17}O_5N_2$ 329.11320, found 329.11298. **9** (*E*-isomer): ^{1}H NMR (300 MHz, $CDCl_3$) δ 7.70–7.20 (m, 3H), 7.14 (d, $J = 16.3$ Hz, 1H), 6.99 (d, $J = 16.3$ Hz, 1H), 6.76 (s, 2H), 3.93 (s, 6H), 3.89 (s, 3H); ^{13}C NMR (75 MHz, $CDCl_3$) δ 153.49, 139.04, 133.03, 131.49, 125.43, 105.93, 104.13, 60.96, 56.14. MS (APCI) *m/z:* 301.1 ($[M4H-2O]^+$), 314.1 ($[M2H-O)^+]$, 329.1 ($[MH]^+$); HRMS calcd for $C_{17}H_{17}O_5N_2$ 329.11320, found 329.11308.

5-(2-Z-Trimethoxyphenylethenyl)benzo[1,2,5]thiadiazole (**14**) *and 5-(2-E-Trimethoxyphenylethenyl) benzo[1,2,5]thiadiazole* (**10**) Purification by flash chromatography (PE/Et_2O, 80:20) afforded 94 % yield of separable isomers *Z/E* (39/61 ratio) (Isomerization of *Z*-isomer during the treatment and purification). **14** (*Z*-isomer): ^{1}H NMR (300 MHz, $CDCl_3$) δ 7.91 (s, 1H), 7.80 (d, $J = 9.1$ Hz, 1H), 7.53 (d, $J = 9.2$ Hz, 1H), 6.72 (s, 2H), 6.49 (s, 2H), 3.85 (s, 3H), 3.63 (s, 6H); ^{13}C NMR (75 MHz, $CDCl_3$) δ 155.13, 154.05, 153.06, 138.99, 137.80, 132.68, 131.82, 131.45, 128.26, 120.96, 120.36, 106.19, 60.94, 55.92; MS (APCI) *m/z:* 329.1 ($[MH]^+$); HRMS calcd for $C_{17}H_{17}O_3N_2S$ 329.09544, found 329.09519. **10** (*E*-isomer): ^{1}H NMR (300 MHz,

$CDCl_3$) δ 7.95 (d, $J = 9.4$ Hz, 1H), 7.94 (s, 1H) 7.86 (d, $J = 9.6$ Hz, 1H), 7.21 (d, $J = 16.2$ Hz, 1H), 7.13 (d, $J = 16.3$ Hz, 1H), 6.79 (s, 2H), 3.93 (s, 6H), 3.89 (s, 3H); ^{13}C NMR (75 MHz, $CDCl_3$) δ 155.48, 154.48, 153.43, 138.55, 132.20, 131.61, 127.78, 126.74, 121.32, 118.65, 103.88, 60.94, 56.12; MS (APCI) *m/z:* 329.1 ([MH]$^+$); HRMS calcd for $C_{17}H_{17}O_3N_2S$ 329.09544, found 329.09513.

*General procedure for the preparation of benzofurazan (**8** and **12**)*

The corresponding *N*-oxidebenzoxadiazole **9** or **13** (0.4 mmol) and triphenylphosphine (93 mg, 0.4 mmol) were dissolved in 30 mL of EtOH and refluxed for 2 h. The solvent was evaporated under reduced pressure and then purified with flash chromatography on silica gel using petroleum ether and AcOEt as eluant to afford benzofurazan in variable yields.

5-(2-E-Trimethoxyphenylethenyl)benzo[1,2-c]1,2,5-oxadiazole (**8**) Purification by flash chromatography (PE/AcOEt, 90:10) afforded pure benzofurazan **8** (85 % yield). ^{1}H NMR (300 MHz, $CDCl_3$) δ 7.81 (d, $J = 9.7$ Hz, 1H), 7.72 (d, $J = 9.5$ Hz, 1H), 7.71 (s, 1H), 7.19 (d, $J = 16.2$ Hz, 1H), 7.06 (d, $J = 16.2$ Hz, 1H), 6.78 (s, 2H), 3.93 (s, 6H), 3.89 (s, 3H); ^{13}C NMR (75 MHz, $CDCl_3$) δ 153.48, 149.76, 148.78, 140.21, 138.94, 133.02, 131.64, 130.10, 126.04, 116.42, 112.54, 104.10, 60.95, 56.14; MS (APCI) *m/z:* 298.1 ([M2H-O)$^+$], 313.1 ([MH]$^+$); HRMS calcd for $C_{17}H_{17}O_4N_2$ 313.11828, found 313.11806.

5-(2-Z-Trimethoxyphenylethenyl)benzo[1,2-c]1,2,5-oxadiazole (**12**) Purification by flash chromatography (PE/AcOEt, 90:10) afforded pure benzofurazan **12** (96 % yield). ^{1}H NMR (300 MHz, $CDCl_3$) δ 7.72 (s, 1H), 7.63 (d, $J = 9.4$ Hz, 1H), 7.28 (d, $J = 9.5$ Hz, 1H), 6.78 (d, $J = 12.1$ Hz, 1H), 6.63 (d, $J = 12.2$ Hz, 1H), 6.45 (s, 2H), 3.86 (s, 3H), 3.67 (s, 6H); ^{13}C NMR (75 MHz, $CDCl_3$) δ 153.13, 149.40, 148.27, 140.94, 138.08, 134.09, 133.95, 131.39, 127.45, 115.15, 114.96, 106.21, 60.92, 55.94; MS (APCI) *m/z:* 313.1 ([MH]$^+$); HRMS calcd for $C_{17}H_{17}O_4N_2$ 313.11828, found 313.11803.

*General procedure for the preparation of benzimidazole 1,3-dioxide derivatives (**11** and **15**)*

The corresponding benzoxadiazole *N*-oxide **9** or **13** (0.22 mmol), 2-nitropropane (23 µL, 1.2 equiv), piperidine (26 µL, 1.2 equiv) in THF (5 mL) were stirred at room temperature until disappearance of starting material was observed by TLC (24–72 h). The solvent was evaporated under reduce pressure. The residue was purified with flash chromatography on silica gel (petroleum ether/AcOEt 50/50 to AcOEt) to afford the corresponding benzimidazole in variable yields.

(E)-2,2-Dimethyl-5-(3,4,5-trimethoxyphenylethenyl)-2H-benzimidazole 1,3-dioxide (**11**) Compound was isolated in 82 % yield. ^{1}H NMR (300 MHz, $CDCl_3$) δ 7.24 (s, 2H), 7.16 (s, 1H), 7.07 (d, $J = 16.2$ Hz, 1H), 6.85 (d, $J = 16.2$ Hz, 1H), 6.73 (s, 2H), 3.92 (s, 6H), 3.88 (s, 3H), 1.73 (s, 6H); ^{13}C NMR (75 MHz, $CDCl_3$) δ 153.44, 139.53, 139.05, 136.46, 135.55, 132.75, 131.56, 129.53, 125.64, 115.65, 111.86, 104.13, 97.42, 60.91, 56.10, 24.11; MS (APCI) *m/z:* 355.2 ([MH-O]$^+$), 371.2 ([MH]$^+$); HRMS calcd for $C_{20}H_{23}O_5N_2$ 371.16015, found 371.16000.

(Z)-2,2-Dimethyl-5-(3,4,5-trimethoxyphenylethenyl)-2H-benzimidazole 1,3-dioxide (**15**) Compound was isolated in 90 % yield. ^{1}H NMR (300 MHz, $CDCl_3$) δ 7.11 (s, 1H), 7.00 (d, $J = 9.7$ Hz, 1H), 6.77 (d, $J = 9.8$ Hz, 1H), 6.71 (d, $J = 12.2$ Hz, 1H), 6.47 (s, 2H), 6.36 (d, $J = 12.2$ Hz, 1H), 3.86 (s, 3H), 3.75 (s, 6H), 1.69 (s, 6H); ^{13}C NMR (75 MHz, $CDCl_3$) δ 153.15, 140.32, 138.25, 136.27, 135.21, 134.40, 132.94, 131.63, 127.24, 114.71, 114.22, 106.37, 104.16, 97.38, 60.96, 56.11, 24.16; MS (APCI) *m/z:* 355.2 ([MH-O]$^+$), 371.2 ([MH]$^+$); HRMS calcd for $C_{20}H_{23}O_5N_2$ 371.16015, found 371.15995.

*General procedure for the preparation of diamine derivatives (**17** and **20**)*

The corresponding benzoxadiazole *N*-oxide **9** or **13** (100 mg, 0.305 mmol) and $SnCl_2{\cdot}H_2O$ (350 mg, 1.52 mmol) in AcOEt (10 mL) were refluxed overnight. Then, the mixture was treated with 10 mL of aqueous solution of $NaHCO_3$ (5 %) and extracted with AcOEt (3 × 10 mL). The organic layer was dried over $MgSO_4$ and evaporated under reduce pressure. The residue was purified with flash chromatography on silica gel (petroleum ether/AcOEt 70/30 to AcOEt) to afford the corresponding benzimidazole in variable yields.

5-(2-E-Trimethoxyphenylethenyl)benzene-1,2-diamine (**17**) Compound was isolated in 79 % yield. ^{1}H NMR (300 MHz, $CDCl_3$) δ 6.98–6.80 (m, 4H), 6.73–6.68 (m, 1H), 6.69 (s, 2H), 3.90 (s, 6H), 3.86 (s, 3H), 3.31 (br s, 4H); ^{13}C NMR (75 MHz, $CDCl_3$) δ 153.25, 137.26, 134.94, 134.59, 133.68, 129.42, 128.41, 125.27, 119.34, 116.52, 114.26, 103.07, 60.88, 55.99.; MS (ESI) *m/z:* 301.2 ([MH]$^+$); HRMS calcd for $C_{17}H_{21}O_3N_2$ 301.15467, found 301.15494.

5-(2-Z-Trimethoxyphenylethenyl) benzene-1,2-diamine (**20**) Compound was isolated in 87 % yield. ^{1}H NMR (300 MHz, $CDCl_3$) δ 6.71–6.66 (m, 2H), 6.59–6.54 (m, 1H), 6.57 (s, 2H), 6.43 (d, $J = 12.2$ Hz, 1H), 6.32 (d,

$J = 12.2$ Hz, 1H), 3.84 (s, 3H), 3.70 (s, 6H), 3.53 (br s, 4H); ^{13}C NMR (75 MHz, $CDCl_3$) δ 152.73, 136.78, 134.20, 134.02, 133.18, 130.13, 128.97, 127.59, 121.39, 117.11, 116.05, 105.87, 60.86, 55.86; MS (APCI) *m/z:* 301.2 ($[MH]^+$); HRMS calcd for $C_{17}H_{21}O_3N_2$ 301.15467, found 301.15498.

*General procedure for the preparation of nitroaniline derivatives (**16**, **18**, and **19**)*

The corresponding benzoxadiazole *N*-oxide **9** or **13** (100 mg, 0.305 mmol) and $FeSO_4.7H_2O$ (6 equiv) in DMSO (10 mL) were stirred for 1 h at room temperature. The mixture was treated with water (10 mL) and extracted with AcOET (3 × 10 mL). The organic layer was dried over $MgSO_4$ and evaporated under reduce pressure. The residue was purified with flash chromatography on silica gel (petroleum ether/AcOEt 80/20) to afford the corresponding benzimidazole in variable yields.

4-(2-E-Trimethoxyphenylethenyl)-2-nitroaniline (**16p**) *and 5-(2-E-Trimethoxyphenylethenyl)-2-nitroaniline* (**16o**) An inseparable mixture of two isomers was isolated in 41 % yield (**16p/16o** 72/28 ratio). ^{13}C NMR (75 MHz, $CDCl_3$) δ 153.42, 153.37, 145.07, 144.49, 143.94, 138.79, 137.85, 133.14, 132.74, 132.01, 131.90, 131.01, 127.49, 126.85, 126.66, 125.88, 123.83, 119.21, 116.23, 114.62, 104.07, 103.31, 60.94, 56.12, 56.07; MS (ESI) *m/z:* 301.2 ($[M3H-2O]^+$), 331.1 ($[MH]^+$), 353.1($[MNa]^+$); HRMS calcd for $C_{17}H_{19}O_5N_2$ 331.12885, found 331.12888. Data for **16p** (NH_2 para (4) ^1H NMR (300 MHz, $CDCl_3$) δ 8.20 (d, $J = 2.0$ Hz, 1H), 7.58 (dd, $J = 8.7$, 2.1 Hz, 1H), 6.90 (s, 2H), 6.82 (d, $J = 8.7$ Hz, 1H), 6.70 (s, 2H), 6.18 (br s, 2H), 3.91 (s, 6H), 3.87 (s, 3H). Data for **16o** (NH_2 ortho (5) ^1H NMR (300 MHz, $CDCl_3$) δ 8.10 (d, $J = 9.0$ Hz, 1H), 7.12 (d, $J = 16.2$ Hz, 1H), 6.90 (s, 1H), 6.89 (d, $J = 9.1$ Hz, 1H), 6.88 (d, $J = 16.2$ Hz, 1H), 6.74 (s, 2H), 6.18 (br s, 2H), 3.91 (s, 6H), 3.88 (s, 3H).

4-(2-Z-Trimethoxyphenylethenyl)-2-nitroaniline (**18**) *and 5-(2-Z-Trimethoxyphenylethenyl)-2-nitroaniline* (**19**) A mixture of two isomers was isolated in 37 % yield of separable isomers 26/27 (80/20 ratio). Isomer 26: ^1H NMR (300 MHz, $CDCl_3$) δ 8.07 (d, $J = 1.8$ Hz, 1H), 7.28 (dd, $J = 9.1$, 2.4 Hz, 1H), 6.63 (d, $J = 8.7$ Hz, 1H), 6.51 (d, $J = 12.2$ Hz, 1H), 6.49 (s, 2H), 6.40 (d, $J = 12.2$ Hz, 1H), 6.13 (br s, 2H), 3.85 (s, 3H), 3.72 (s, 6H); ^{13}C NMR (75 MHz, $CDCl_3$) δ 153.10, 143.66, 137.35, 136.42, 132.42, 131.70, 129.82, 127.58, 126.45, 126.27, 118.17, 105.78, 60.95, 55.98; MS (APCI) *m/z:* 331.1 ($[MH]^+$); HRMS calcd for $C_{17}H_{19}O_5N_2$ 331.12885, found 331.12871. Isomer 27: ^1H NMR (300 MHz, $CDCl_3$) δ 8.00 (d, $J = 8.9$ Hz, 1H), 6.73 (s, 1H), 6.63 (dd, $J = 8.9$, 1.7 Hz, 1H),, 6.65 (d, $J = 12.2$ Hz, 1H), 6.48 (s, 2H), 6.43 (d, $J = 12.2$ Hz, 1H), 6.21 (br s, 2H), 3.85 (s, 3H), 3.70 (s, 6H); ^{13}C NMR (75 MHz, $CDCl_3$) δ 153.02, 145.22, 133.40, 131.46, 127.63, 126.02, 118.39, 118.09, 106.12, 60.96, 55.98; MS (APCI) *m/z:* 331.1 ($[MH]^+$); HRMS calcd for $C_{17}H_{19}O_5N_2$ 331.12885, found 331.12860.

Cell models and in vitro treatments

The histological types and origins of the three cancer cell lines that were used for the MTT colorimetric assay are as follows. The cell lines were obtained from the American Type Culture Collection (ATCC, Manassas, VA), the European Collection of Cell Culture (ECACC, Salisbury, UK), and the Deutsche Sammlung von Mikroorganismen und Zellkulturen (DSMZ, Braunschweig, Germany). The analyzed cell lines include the U373 (ECACC code 89081403) glioma, the LoVo (DSMZ code ACC350) colon carcinoma, and the PC-3 (ATCC code CRL1435) prostate carcinoma cell lines. All cell lines are from human origin. The cancer cell lines were cultured in DMEM. Human Umbilical Vein Endothelial cells (HUVECs, Sigma-Aldrich) were cultured in endothelial cell growth medium (Sigma), in 0.2 % gelatinized plates. After 24-h period of incubation at 37 °C, the tested compounds (dissolved in sterile DMSO) are diluted in culture medium in order to have a 10× concentration. The dilutions are made in a 96-well plate with a round bottom. Twenty microlitre of each dilution is mixed with the 180 µL of culture medium in the appropriate well. The final concentrations are 10^{-8}, 5.10^{-8}, 10^{-7}, 5.10^{-7}, 10^{-6}, 5.10^{-6}, 10^{-5}, 5.10^{-5}, and 10^{-4} g/mL. Each experiment is made with an n = 6. Cells are incubated in a humidified atmosphere and a CO_2 concentration fixed at 5 % in a Binder incubator. After 72-h incubation at 37 °C, with or without the compound to be tested, the medium was replaced by 100 µL of HBSS (without phenol red) containing MTT at the concentration of 1 mg/mL. The micro-wells are subsequently incubated during 3 h at 37 °C and centrifuged at 1600 rpm during 4 min. Medium is removed, and formazan crystal formed is dissolved in 100 µL non-sterile DMSO. The plate is incubated in the dark during 10 min. The micro-wells are shaken for 1 min and read on a spectrophotometer at wavelengths of 570 nm (maximum of formazan absorbance) and 650 nm (background). For each experimental condition, the mean optical density is calculated, allowing the determination of the percentage of living cells in comparison with the control.

Metabolic stability studies

Compounds at 10 µM (stock solution in DMSO at 5 mM) were preincubated at 37 °C for 5 min in tubes with NADPH regenerating system (1.3 mM NADP, 3.3 mM

D-glucose 6-phosphate, 3.3 mM $MgCl_2$, and 0.4 U/mL glucose-6-phosphate dehydrogenase) in 0.1 M potassium phosphate buffer pH 7.4 (BD Biosciences, Woburn, MA). The reaction was initiated by the addition of pooled human liver S9 or pooled mouse liver microsomes (1 mg protein/mL, BD Biosciences, Woburn, MA). Aliquots (100 µL) were removed at 0, 10, 30, 60, and 120 min and mixed with 100 µL acetonitrile, vortexed, and centrifuged for 5 min at 10,000 rpm. The supernatants were then subjected to UV–HPLC analysis. Controls consisted of: (a) incubation of tested compound (positive control) in 0.1 M potassium phosphate buffer and (b) incubation of all components except NADPH regenerating system. All incubations were assayed in duplicate.

UV–HPLC analysis

Methanol HPLC grade was purchased from Prolabo, VWR (Leuven, Belgium), and acetonitrile HPLC grade from Fisher Scientific (Tournai, Belgium). Analysis was performed on a LaChrom Elite HPLC integrated system (Merck Hitachi, VWR, Leuven, Belgium) equipped with a L-2450 UV detector, a L-2300 oven, L-2130 autosampler, and L-2130 pump all piloted by EZChrom software. Chromatographic experiments were carried out in isocratic mode on a RP-18e 250 mm × 4 mm LiChroCART® column (5 µM) equipped with a guard column. The mobile phase consisted of a mixture of acetonitrile and water in isocratic mode (see Table 5). The flow rate was 1 mL/min, and the injected volume was 20 µL. Analysis was carried out at room temperature at different wavelengths (see Table 5). To determine metabolic stability, results were expressed as the remaining percentage of compound against time by dividing the peak area of test compound at each time point by the peak area at 0 min multiplied by 100. The slope of the linear regression from log percentage remaining versus incubation time relationships (-k) was used to calculate the in vitro half-life ($t_{1/2}$) of compounds by the formula of in vitro $t_{1/2} = \ln(2)/k$, regarded as first-order kinetics (GraphPad Prism, version 5). *In vitro* intrinsic clearance (CL_{int}) of compounds was calculated using the formula $CL_{int} = (\ln(2)/t_{1/2}) \times (V/P)$, where V is the incubation volume, and P is the mass of microsomal proteins in the incubation mixture.

Metabolite identification

For metabolites identification, chromatographic experiments were carried out in gradient mode in order to separate each newly formed metabolite. Mobile phases were A: 0.1 % trifluoroacetic acid in water and B: 0.1 % trifluoroacetic acid in acetonitrile. Gradient elution was from 20 to 100 % phase B in 20 min and 5 min at 100 % B at 1 mL/min on a RP-18e 250 mm × 4 mm LiChroCART® column (5 µM) equipped with a guard column. Metabolites identification was performed by LC–MS analysis on an Accela HPLC system hyphenated with a LTQ-Orbitrap XL mass spectrometry system (Thermo Fisher Scientific, Bremen, Germany) from UCL MASS-MET platform. The system was equipped with an APCI interface that was used in positive ionization. Identification of major metabolites was achieved by comparing their retention time and mass spectra (MS and MS^2) with synthetic metabolic standards.

Cell treatment for caspase-3 activation

U373 (human brain tumor cells), plated in a P60 at full confluence, were treated with the compounds at the given concentrations. After a 24-h treatment, the cells were lysed with ripa buffer containing proteases inhibitors.

Immunoblot anti-caspase 3

Cell extracts were separated by SDS–PAGE and transferred onto PVDF membranes before incubation with

Table 5 HPLC conditions (mobile phase and wavelength of detection) for each compound

Compound	Mobile phase (v/v)	Wavelength (nm)
8	ACN/H_2O 60/40	298
9	ACN/H_2O 60/40	313
10	ACN/H_2O 70/30	298
11	ACN/H_2O 40/60	365
12	ACN/H_2O 60/40	277
13	ACN/H_2O 60/40	258
14	ACN/H_2O 70/30	298
15	ACN/H_2O 40/60	292

primary antibody as previously described (Seront *et al.*, 2013). Antibody against total and active caspase-3 was purchased from Cell Signaling (Danvers, MA, USA).

Flow cytometry

U373 cells (ECACC catalogue number 08061901) were seeded in T25 flasks and treated with compounds at the given concentrations during 72 h. A the end of the treatment periods, cells were detached with trypsin–EDTA, pooled with their supernatant, centrifuged, washed with PBS, and fixed for 1 h in paraformaldehyde 1 % in PBS at 4 °C. After permeabilization overnight with 70 % ice-cold ethanol, cells were stained by TUNEL technic as well as propidium iodide with the APO AF apoptosis detection kit according to the manufacturer's instructions (BD, Erembodegem, Belgium). Cells were then analyzed for their fluorescence levels with a Cell Lab Quanta flow cytometer (Beckman Coulter, ANalis, Suarlee, Belgium). MCF7 breast cancer cells (DSMZ code ACC115) left untreated or treated with 1 μM narciclasine for 72 h were used as negative and positive controls (Dumont *et al.*, 2007). Experiment was conducted once in tetraplicate, and results are presented as mean ± SEM.

Acknowledgments The authors thank Dr. Marie-France Hérent for her skillful assistance on the MASSMET platform. The authors gratefully thank the Région Bruxelles-Capitale (INNOVIRIS) for financial support on this research. This work was supported by the Fonds National de la Recherche Scientifique (F.R.S.-FNRS, Belgium) FRFC Grant No. 2.4555.08 and the Fonds Spécial de Recherche (FSR) of the Faculty of Medecine (UCL) as part of the MASSMET platform (LC-HRMS Orbirtap).

References

Abu El-Haj MJ (1972) Novel synthesis of 1-hydroxy-1H-benzimidazole 3-oxides and 2,2-dialkyl-2H-benzimidazole 1,3-dioxides. J Org Chem 37:2519–2520

Aguirre G, Boiani L, Boiani M, Cerecetto H, Di Maio R, Gonzalez M, Porcal W, Denicola A, Piro OE, Castellano EE, Sant'Anna CMR, Barreiro EJ (2005) New potent 5-substituted benzofuroxans as inhibitors of Trypanosoma cruzi growth: quantitative structure–activity relationship studies. Bioorg Med Chem 13:6336–6346

Bedford SB, Quarterman CP, Rathbone DL, Slack JA, Griffin RJ, Stevens MFG (1996) Synthesis of water-soluble prodrugs of the cytotoxic agent combretastatin A4. Bioorg Med Chem Lett 6:157–160

Boiani M, Boiani L, Denicola A, Torres de Ortiz S, Serna E, Vera de Bilbao N, Sanabria L, Yaluff G, Nakayama H, Rojas de Arias A, Vega C, Rolan M, Gomez-Barrio A, Cerecetto H, Gonzalez M (2006) 2H-benzimidazole 1,3-dioxide derivatives: a new family of water-soluble anti-trypanosomatid agents. J Med Chem 49:3215–3224

Carroll WA, Altenbach RJ, Bai H, Brioni JD, Brune ME, Buckner SA, Cassidy C, Chen Y, Coghlan MJ, Daza AV, Drizin I, Fey TA, Fitzgerald M, Gopalakrishnan M, Gregg RJ, Henry RF, Holladay MW, King LL, Kort ME, Kym PR, Milicic I, Tang R, Turner SC, Whiteaker KL, Yi L, Zhang H, Sullivan JP (2004) Synthesis and structure–activity relationships of a novel series of 2,3,5,6,7,9-hexahydrothieno[3,2-b]quinolin-8(4H)-one 1,1-dioxide K(ATP) channel openers: discovery of (-)-(9S)-9-(3-bromo-4-fluorophenyl)-2,3,5,6,7,9-hexahydrothieno[3,2-b]quinolin-8(4H)-one 1,1-dioxide (A-278637), a potent K(ATP) opener that selectively inhibits spontaneous bladder contractions. J Med Chem 47:3163–3179

Chaplin DJ, Dougherty GJ (1999) Tumour vasculature as a target for cancer therapy. Br J Cancer 80(Suppl 1):57–64

Collins JA, Schandi CA, Young KK, Vesely J, Willingham MC (1997) Major DNA fragmentation is a late event in apoptosis. J Histochem Cytochem Off J Histochem Soc 45:923–934

Cushman M, Nagarathnam D, Gopal D, He HM, Lin CM, Hamel E (1992) Synthesis and evaluation of analogues of (Z)-1-(4-methoxyphenyl)-2-(3,4,5-trimethoxyphenyl)ethene as potential cytotoxic and antimitotic agents. J Med Chem 35:2293–2306

Dark GG, Hill SA, Prise VE, Tozer GM, Pettit GR, Chaplin DJ (1997) Combretastatin A-4, an agent that displays potent and selective toxicity toward tumor vasculature. Cancer Res 57:1829–1834

DaSilveira Neto BA, Lopes AS, Ebeling G, Gonçalves RS, Costa VEU, Quina FH, Dupont J (2005) Photophysical and electrochemical properties of π-extended molecular 2,1,3-benzothiadiazoles. Tetrahedron 61:10975–10982

Dumont P, Ingrassia L, Rouzeau S, Ribaucour F, Thomas S, Roland I, Darro F, Lefranc F, Kiss R (2007) The Amaryllidaceae isocarbostyril narciclasine induces apoptosis by activation of the death receptor and/or mitochondrial pathways in cancer cells but not in normal fibroblasts. Neoplasia 9:766–776

Jänicke RU, Ng P, Sprengart ML, Porter AG (1998) Caspase-3 is required for alpha-fodrin cleavage but dispensable for cleavage of other death substrates in apoptosis. J Biol Chem 273:15540–15545

Liekens S, De Clercq E, Neyts J (2001) Angiogenesis: regulators and clinical applications. Biochem Pharmacol 61:253–270

Maya ABS, Pérez-Melero C, Mateo C, Alonso D, Fernandez JL, Gajate C, Mollinedo F, Pelaez R, Caballero E, Medarde M (2005) Further naphthylcombretastatins. An investigation on the role of the naphthalene moiety. J Med Chem 48:556–568

Nam N-H (2003) Combretastatin A-4 analogues as antimitotic antitumor agents. Curr Med Chem 10:1697–1722

Nathan P, Zweifel M, Padhani AR, Koh DM, Ng M, Collins DJ, Harris A, Carden C, Smythe J, Fisher N, Taylor NJ, Stirling JJ, Lu SP, Leach MO, Rustin GJS, Judson I (2012) Phase I trial of combretastatin A4 phosphate (CA4P) in combination with bevacizumab in patients with advanced cancer. Clin Cancer Res Off J Am Assoc Cancer Res 18:3428–3439

Ohsumi K, Nakagawa R, Fukuda Y, Hatanaka T, Morinaga Y, Nihei Y, Ohishi K, Suga Y, Akiyama Y, Tsuji T (1998) Novel combretastatin analogues effective against murine solid tumors: design and structure–activity relationships. J Med Chem 41:3022–3032

Pettit GR, Singh SB, Boyd MR, Hamel E, Pettit RK, Schmidt JM, Hogan F (1995a) Antineoplastic agents. 291. Isolation and synthesis of combretastatins A-4, A-5, and A-6(1a). J Med Chem 38:1666–1672

Pettit GR, Temple C Jr, Narayanan VL, Varma R, Simpson MJ, Boyd MR, Rener GA, Bansal N (1995b) Antineoplastic agents 322. Synthesis of combretastatin A-4 prodrugs. Anticancer Drug Des 10:299–309

Porcal W, Merlino A, Boiani M, Gerpe A, Gonzalez M, Cerecetto H (2008) Arylethenylbenzofuroxan derivatives as drugs for chagas disease: multigram batch synthesis using a Wittig–Boden process ‡. Org Process Res Dev 12:156–162

Poulain R, Horvath D, Bonnet B, Eckhoff C, Chapelain B, Bodinier MC, Déprez B (2001) From hit to lead. Combining two

complementary methods for focused library design. Application to mu opiate ligands. J Med Chem 44:3378–3390

Rustin GJS, Galbraith SM, Anderson H, Stratford M, Folkes LK, Sena L, Gumbrell L, Price PM (2003) Phase I clinical trial of weekly combretastatin A4 phosphate: clinical and pharmacokinetic results. J Clin Oncol Off J Am Soc Clin Oncol 21:2815–2822

Seront E, Boidot R, Bouzin C, Karroum O, Jordan BF, Gallez B, Machiels JP, Feron O (2013) Tumour hypoxia determines the potential of combining mTOR and autophagy inhibitors to treat mammary tumours. Br J Cancer 109:2597–2606. doi:10.1038/bjc.2013.644

Simoni D, Romagnoli R, Baruchello R et al (2006) Novel combretastatin analogues endowed with antitumor activity. J Med Chem 49:3143–3152

Simoni D, Romagnoli R, Baruchello R, Rondanin R, Grisolia G, Eleopra M, Rizzi M, Tolomeo M, Giannini G, Alloatti D, Castorina M, Marcellini M, Pisano C (2008) Novel A-ring and B-ring modified combretastatin A-4 (CA-4) analogues endowed with interesting cytotoxic activity. J Med Chem 51:6211–6215

Zweifel M, Jayson GC, Reed NS, Osborne R, Hassan B, Ledermann J, Shreeves G, Poupard L, Lu SP, Balkissoon J, Chaplin DJ, Rustin GJS (2011) Phase II trial of combretastatin A4 phosphate, carboplatin, and paclitaxel in patients with platinum-resistant ovarian cancer. Ann Oncol Off J Eur Soc Med Oncol 22:2036–2041